Am J Physiol Renal Physiol 305: F295–F303, 2013.
First published May 29, 2013; doi:10.1152/ajprenal.00527.2012.

Feline chronic kidney disease is associated with shortened telomeres and increased cellular senescence

Jessica M. Quimby,[1] David G. Maranon,[2] Christine L. R. Battaglia,[2] Shannon M. McLeland,[3] William T. Brock,[1] and Susan M. Bailey[2]

[1]*Department of Clinical Sciences, College of Veterinary Medicine and Biomedical Sciences, Colorado State University, Fort Collins, Colorado;* [2]*Department of Environmental and Radiological Health Sciences, Colorado State University, Fort Collins, Colorado; and* [3]*Department of Molecular Biology, Immunology and Pathology, Colorado State University, Fort Collins, Colorado*

Submitted 13 September 2012; accepted in final form 28 May 2013

Quimby JM, Maranon DG, Battaglia CL, McLeland SM, Brock WT, Bailey SM. Feline chronic kidney disease is associated with shortened telomeres and increased cellular senescence. *Am J Physiol Renal Physiol* 305: F295–F303, 2013. First published May 29, 2013; doi:10.1152/ajprenal.00527.2012.—Telomeres are protective structures at the ends of chromosomes that have important implications for aging. To address the question of whether telomeres contribute to feline chronic kidney disease (CKD), we evaluated kidney, liver, and skin samples from 12 cats with naturally occurring CKD, 12 young normal cats, and 6 old normal cats. Telomere length was assessed using standard telomere fluorescent in situ hybridization (TEL-FISH) combined with immunohistochemistry (TELI-FISH) to identify proximal (PTEC) and distal tubular epithelial cells (DTEC), whereas senescence-associated β-galactosidase (SABG) staining was used to evaluate senescence. Results revealed statistically significant decreases in the average telomere fluorescence intensity (TFI) of PTEC in CKD cats compared with young and geriatric normal cats, and in the DTEC of CKD cats compared with young normal cats. When histograms of individual TFI were compared, statistically significant decreases in the PTEC and DTEC of CKD cats were observed compared with young and geriatric normal cats. Concomitantly, a statistically significant increase in SABG staining was seen in CKD kidney samples compared with young normal cats. CKD cats tended to have increased SABG staining in the kidney compared with normal geriatric cats, but this did not reach statistical significance. No significant telomere shortening in liver or skin from any group was observed. Real-time quantitative telomeric repeat amplification protocol assessment of renal telomerase activity revealed comparable low levels of telomerase activity in all groups. Our results suggest that shortened telomeres and increased senescence in the kidneys of CKD cats may represent novel targets for interventional therapy.

kidney; telomere; senescence; feline; aging

CHRONIC KIDNEY DISEASE (CKD) is a common naturally occurring medical condition in elderly cats, yet an etiology for this disease process has not been elucidated (2). Human CKD is associated with progressive loss of renal parenchyma and function with age (37). Renal aging also involves loss of an appropriate response toward injury, as seen in aging human populations where kidney injury is more common and clinically more severe, and kidney function is less likely to recover (43). Whether feline CKD results from similar aging processes that predispose the organ to failure or whether other factors are involved remains to be determined.

Address for reprint requests and other correspondence: J. Quimby, Dept. of Clinical Sciences, Colorado State Univ., Fort Collins, CO 80523 (e-mail: jquimby@colostate.edu).

Telomeres are protective structures that serve to cap chromosome ends and so are critical for maintaining genome stability (18, 36). Telomeres prevent natural chromosomal termini from being identified as double-strand break (DSB) ends, thereby abrogating a DNA damage response that would result in cell cycle arrest, apoptosis, or death (18, 49). Additionally, in the absence of sufficient telomerase activity for de novo telomere addition or an alternative telomere maintenance mechanism to counter the "end replication problem," telomeres shorten with each cycle of replication (18). Other factors also contribute to telomere shortening, including deletions and oxidative stress (18, 49).

When telomeres reach a critically shortened state, they are no longer able to effectively cap the end of the chromosome, and so they themselves are detected as DNA damage and trigger a response resulting in permanent cell cycle arrest known as cellular senescence (18, 49). Most human tissues have been shown to experience telomere shortening with age, and shortened telomeres have been associated with a variety of disease states (16, 45, 49). Interestingly, increased cellular senescence has been documented in human renal disease conditions and so may play an important role in susceptibility to injury in the aging kidney (32, 34, 37, 48). Telomeres are acutely sensitive to oxidative stress, partly due to their high content of guanine residues but also because telomeres are deficient in repair of the DNA damage caused by reactive oxygen species (ROS) (16). Associations between oxidative stress, telomere shortening, and inflammation have also been suggested, making investigation of telomere maintenance particularly pertinent for inflammatory disease conditions (16, 28, 41). Feline CKD represents an ideal model for such studies, since it is a naturally occurring disease characterized by tubulointerstitial inflammation (6), and decreased antioxidant defense mechanisms and increased oxidative stress have been documented in these patients (21, 50).

Very few prior studies have evaluated telomere length and telomerase activity in cats. No evidence of significant telomerase activity has been reported in a variety of normal feline tissues including liver, spleen, kidney, lung, heart, brain, muscle, skin, mammary tissue, and ovaries of young cats using traditional telomeric repeat amplification protocol (TRAP) assay technology (4, 9, 29). Feline peripheral blood mononuclear cell (PBMC) telomeres have been reported to vary in signal intensity between homologs (14) and significantly decrease in length with age (29). Telomere length has not been previously assessed in the feline kidney or in feline CKD.

The purpose of the present study was to assess telomere length and cellular senescence in feline CKD. Telomere length in cat kidney sections was analyzed on a cell-by-cell basis using a novel approach that combined telomere fluorescence in situ hybridization with immunostaining (TELI-FISH) to identify and distinguish specific cellular compartments of interest (i.e., the proximal tubule), and to avoid other cells that may be present (e.g., inflammatory infiltrates) (30). We hypothesized that shortened telomeres and increased cellular senescence would be observed in the kidneys of geriatric cats affected by CKD compared with liver or skin, and compared with young or old normal cats. Telomerase activity in kidney and liver tissues was also assessed utilizing the sensitive real-time quantitative TRAP assay (RTQ-TRAP). Demonstration of an association between telomere shortening, cellular senescence, and feline CKD would serve to further our understanding of renal aging and disease, and have the potential to present novel treatment strategies, with the cat serving as an informative translational model of this naturally occurring disease.

MATERIALS AND METHODS

Sample Collection

Samples were collected from the three study groups: 12 cats with CKD; 12 young normal cats; and 6 geriatric cats without evidence of CKD. Kidney, liver, and skin samples were collected in formalin for histopathology and TELI-FISH analysis, as well as quick frozen in optimal cutting temperature (OCT) media (Sakura Finetek, Torrance, CA) for senescence-associated β-galactosidase (SABG) staining. The study was approved by the Institutional Animal Care and Use Committee at Colorado State University.

FISH Slide Preparation

Deparaffinization (kidney, liver, and skin). Kidney and liver samples were cut from paraffin blocks at a thickness of 2 μm; skin samples were cut at 3 μm. Slides were incubated at 65°C (10 min), followed by three xylene washes (10 min). Slides were dehydrated through a graded ethanol series and rinsed in PBS, then immersed in 3% hydrogen peroxide (5 min), washed in PBS, immersed in methanol (5 min), and washed in PBS. Kidney samples that were undergoing antigen retrieval before TELI-FISH were immersed in 3% paraformaldehyde (10 min).

Antigen retrieval (kidney). Kidney samples were prepared for TELI-FISH by immersing in citrate buffer (Dako, Carpinteria, CA) and steaming at 125°C (1 min) in a pressure cooker. Slides were rinsed with deionized (DI) water, dehydrated through a graded ethanol series, and stored at 4°C.

TEL-FISH (liver and skin). Slides were immersed in 1% Tween-20 detergent (60 s; Sigma Aldrich, St. Louis, MO) and rinsed briefly in DI water. Proteinase K (100 μl of 100 mcg/ml; Roche, San Francisco, CA) was applied to slides, which were coverslipped and incubated at 37°C (15 min). Slides were washed in PBS (2 min) and dehydrated through a graded ethanol series, then air-dried. A Cy3-labeled peptide nucleic acid (PNA) telomere probe ($TTAGGG_3$, Biosynthesis, Lewisville, TX) was prepared by diluting 5 μl of probe in 36 μl of formamide (Sigma Aldrich), 12 μl of 0.05 M TRIS buffer, 2.5 μl of 0.1 M KCl (Sigma Aldrich), and 0.6 μl of 0.1 M MgCl (Sigma Aldrich) for a final concentration of 300 ng/ml. Probe mix (50 μl) was applied to each slide, which was then coverslipped and denatured at 85°C (5 min). Slides were incubated at 37°C for 2 h, then washed in a series of 43.5°C washes for 2.5 min each; washes 1/2: 50% formamide in 2× sodium citrate (SSC); washes 3/4: 2× SSC; and washes 5/6: 2× SSC + 0.1% NP40. Slides were counterstained with 50 μl of DAPI (in Prolong Gold Antifade, Invitrogen, Carlsbad, CA), coverslipped, then stored at −20°C. Slides were processed in sets of three, one sample from each group, to limit variability between sample runs.

TELI-FISH (kidney). Slide preparation was as above, except following telomere probe hybridization, slides were incubated (2 h at room temperature) sequentially with two primary antibodies (concentration of 1:300); aquaporin 1(mouse anti-Aquaporin 1, Millipore, Billerica, MA) to identify proximal tubule segments and cytokeratin AE1/AE3 (rabbit anti-cytokeratin, Cell Marque, Rocklin, CA) to identify distal proximal tubule segments (3, 40). Anti-mouse-Alexa 488 and anti-rabbit-Alexa 647 secondary antibodies (Invitrogen, Carlsbad, CA) were applied (concentration of 1:750; 30 min at room temperature) to visualize aquaporin 1 (green) and cytokeratin (red); slides were washed as above at 43.5°C.

FISH Image Capture and Processing

Image Z stacks were acquired using a Nikon Eclipse 600 microscope outfitted with a Coolsnap ES camera and running Metamorph software (Molecular Devices, Sunnyvale, CA). For each cell population (renal proximal tubule, renal distal tubule, liver, and skin), 15–20 composite images were created from 26 individual stacks (0.2 μm/plane) in two different wavelengths (Dapi and Cy3); three-dimensional (3D) deconvolution was performed using Image J software under 3D blind parameters (available as a download from http://rsb.info.nih.gov/ij/). In addition; PSF (point spread function) was calculated for each picture to obtain a maximum projection of the stacks, allowing visualization and analysis of telomere signals throughout the entirety each cell nuclei.

FISH Data Analysis with TELOMETER

Analysis of TFI was performed using TELOMETER, available as a download from http://demarzolab.pathology.jhmi.edu/telometer/downloads/index.html. Telomere signals from 60 nuclei/sample were analyzed using custom program settings (minimum object size: 1; maximum object size: 350; despeckle ratio: 0.3; rolling ball size: 1). Mean sample TFI was calculated and individual TFI frequency histograms were created for each sample group using Prism software (Prism 5, GraphPad, La Jolla, CA). Mean sample TFI for kidney, liver, and skin from all three groups of cats were statistically compared using one-way ANOVA with Dunn's post hoc analysis in Prism 5 software. Finite mixed-model analysis was performed on individual TFI histograms using SAS software (SAS 9.3, SAS Institute, Cary, NC).

SABG Slide Preparation

Kidney and liver samples were collected in OCT media at the time of death and stored at −80°C until analysis. OCT blocks were cryosectioned at 4 μm (Leica CM 1850, Leica Microsystems, Wetzlar, Germany) and stored at −20°C until analysis. SABG staining was performed using a commercially available kit for assessment of cellular senescence (no. 9860, Cell Signaling Technology, Danvers, MA), which is based on the Dimri protocol (7). β-Galactosidase was prepared fresh for each sample run, and 4 μl of HCL were added (final pH of 6.0); 200 μl were applied per slide, which was coverslipped, sealed with rubber cement, and incubated at 37°C for 14 h. Slides were rinsed in DI, counterstained with eosin, dehydrated, and mounted with xylene mounting media before analysis.

SABG Image Capture and Analysis

Image capture was performed using a Zeiss microscope outfitted with a Coolsnap ES camera. Four images of the renal cortex or liver parenchyma were obtained from each sample. Image analysis was performed using AxioVision software (Carl Zeiss MicroImaging, Jena, Germany). Statistical analysis was performed using a one-way ANOVA with Dunn's post hoc analysis in Prism 5 software.

RTQ-TRAP Telomerase Assay and Analysis

Kidney and liver samples (a subset of five samples from each group) were collected and flash frozen in liquid nitrogen within 2 h of death and stored at −80°C until analysis. The SYBR Green RTQ-TRAP assay was adapted from Hou et al. and Herbert et al. (13, 15). Samples were weighed (20–30 mg), suspended in cold M-PER lysis buffer (Thermofisher, Lafayette, CO) with protease inhibitor (Roche, Indianapolis, IN) and ribonuclease inhibitor (25 μl/100 μl lysis buffer; Promega, Madison, WI) at the ratio of 100 μl per 10 mg of sample. Protein extraction was performed using a glass-on-glass homogenizer on ice. Following homogenization, samples were immediately refrozen on dry ice and moved to −80°C within 1 h. The lysate was processed using RNase-free conditions. Briefly, the sample was thawed on ice and centrifuged at 13,000 rcf at 4°C for 10 min. The supernatant was removed, and the sample was centrifuged once more at 13,000 rcf at 4°C for 10 min to ensure complete removal of cellular debris. Lysates were aliquoted and refrozen at −80°C. Each sample was not freeze-thawed more than three times. Protein content was determined using a Bradford protein assay (Bio-Rad, Hercules, CA).

The SYBR green master mix (Bio-Rad) included all necessary dNTPs, $MgCl_2$, enzyme, and Sybr green to complete the RTQ-PCR reaction. Each well contained 0.5 μg of protein lysate (0.25 μg for Hela cell lysate, the experimental control), 50% volume of SYBR green master mix, 0.2 μg T4 gene32 protein (New England Biolabs, Ipswitch, MA), 0.1 μg of each primer TS (5′-AATCCGTCGAGCAGAGTT-3′) and ACX [5′-GCGCGG(CTTACC)$_3$CTAACC-3′] (Integrated DNA Technologies, Coralville, IA) and RNase/DNase free water to achieve a final well volume of 25 μl. The samples were loaded into a real-time 96-well microtiter plate (Thermofisher, Lafayette, CO) and sealed with a real-time PCR sealant film (Thermofisher, Lafayette, CO). The PCR and detection was performed on a CFX 96 (Bio-Rad). In addition to the treatment samples, a series of controls were also included on each plate: *1*) no template control with TS primer only, *2*) no template control with ACX primer only, *3*) no template control with TS and ACX primers, *4*) heat-inactivated control with template (protein lysate) and TS and ACX primers, and *5*) HeLa cell lysate with TS and ACX primers (a positive control robust in telomerase).

The RTQ-PCR program includes the following steps: *step 1*: 1 cycle at 25°C for 20 min (used to allow telomerase in the protein extracts to elongate the TS primer by adding TTAGGG repeat sequences to it); *step 2*: 1 cycle at 95°C for 3 min (provides heat activation of the enzyme in the SYBR master mix); *step 3*: 40 cycles at 95°C for 20 s, 50°C for 30 s, and 72°C for 90 s (PCR amplification of already elongated TS oligo, allows for detection by real-time instrument); *step 4*: 80 cycles for 0.10 s per cycle (melt curve, ensures no primer dimer formation). The more telomerase activity in the sample, the more rapidly the threshold of amplification (Ct) is achieved. Each sample is run in triplicate on a 96-well plate format allowing for an average Ct to be obtained per sample. Utilizing the average Ct value, the relative percent telomerase activity in each sample is calculated using the Livak method, or Delta Delta Ct method ($2^{-\Delta\Delta Ct}$) (38). Briefly, to calculate the percent relative activity for each sample, one must first normalize the average Ct for a sample to the no template control with TS and ACX primers (control run on each plate). This is referred to as the delta Ct value. The delta Ct value of one sample is then subtracted from the delta Ct value of the chosen comparative sample, yielding a delta delta Ct value ($\Delta\Delta Ct$). Using the $2^{-\Delta\Delta Ct}$, a relative value is generated for each sample comparison and, when multiplied by 100, is the relative percent of telomerase activity in *sample A* compared with *sample B*. A percent value can then be compared between samples assayed across different plates.

Results from the two runs were averaged and normalized to the average telomerase activity for each tissue from young normal cats, and a one-way ANOVA with Dunn's post hoc comparison (Graphpad Prism 5, La Jolla, CA) was performed to determine significant differences between groups.

RESULTS

Categorization of Study Groups and Sample Collection

CKD was defined as a cat with a clinical pathology history of a urine specific gravity of <1.035 and a creatinine of over 2.0 mg/dl. The CKD study group consisted of eight domestic short hairs (DSH), three Siamese crosses, and 1 Ragdoll (total of 12) with a mean age of 14.8 yr (range 6–19 yr); four were neutered males and eight were spayed females. Median serum creatinine was 4.4 mg/dl (range 1.6–9.5 mg/dl), and median urine specific gravity was 1.015 (range 1.010–1.025).

Young normal cats were defined by physical exam findings of healthy body condition and minimal dental tartar, and a normal complete blood count, chemistry, and urinalysis (urine specific gravity of >1.035); cats were acquired from local humane societies where they had been euthanized as unwanted pets. The young, normal study group consisted of 11 DSH and 1 domestic long hair (total of 12), with a mean age of 2.7 yr (range 0.8–4 yr); 4 were neutered males, 2 were intact males, 5 were spayed females, and 1 was an intact female. Median serum creatinine was 1.2 mg/dl (range 0.8–1.5 mg/dl), and median urine specific gravity was 1.067 (range 1.048–1.084).

Geriatric normal cats were defined as those with no clinical history of CKD, a urine specific gravity of >1.035, and minimal changes on renal histopathology. For the geriatric normal study group, the goal was 12, but elderly cats without renal compromise were very difficult to obtain. Therefore, tissues from six geriatric DSH cats with a mean age of 11.5 yr (range 10–16 yr) without CKD were collected; four were spayed females, and two were neutered males. Median serum creatinine was 1.2 mg/dl (range 0.6–1.4 mg/dl), and median urine specific gravity was 1.055 (range 1.047–1.060).

Kidney, liver, and skin samples were collected from the three study groups; all were assessed histopathologically to confirm that kidney samples were appropriately categorized and that liver and skin samples were normal. Sections of kidneys consisted of cortex, medulla, and renal pelvis and were categorized into the following groups: normal, normal geriatric, and CKD cats. Normal geriatric cats were determined based on either absence of histological abnormalities or very mild, scattered, cortical interstitial mononuclear infiltrates with occasional tubular and glomerular basement membrane thickening. In contrast, typical CKD cats had severe interstitial infiltrates in conjunction with fibrosis, tubular loss, degeneration, and glomerulosclerosis. Normal cats, in contrast, lacked such histological changes. Sections of liver from study cats were assessed for the presence of metastatic or primary hepatic neoplasia, inflammation, or hepatopathy. Sections of skin from study cats were assessed for the presence of neoplasia or dermatopathy. Patients were excluded based on the presence of inflammatory disease and/or neoplasia. Only one potential case was excluded due to hepatopathy. All skin sections examined were histologically normal.

Telomeres are Significantly Shortened in Kidneys of CKD Cats

TELI-FISH was optimized for felines and used to definitively identify two cellular compartments within the renal cortex for cell-by-cell telomere length analysis. (Fig. 1, *A* and *B*). Loss of proximal tubule segments was readily apparent in CKD samples. There was a statistically significant decrease in the average telomere fluorescence intensity (TFI) of proximal tubular epithelial cells (PTEC) of CKD cats compared with either young normal or geriatric normal cats ($P = 0.0007$) (Fig. 1*C*). There was a statistically significant decrease in the average TFI in the distal tubular epithelial cells (DTEC) of CKD cats compared with young normal cats ($P = 0.004$) (Fig. 1*D*). No significant difference in average TFI was found between young normal and geriatric normal cats for either cell population. It was also noted that background autofluorescence was more prominent in young normal cat samples than in other groups.

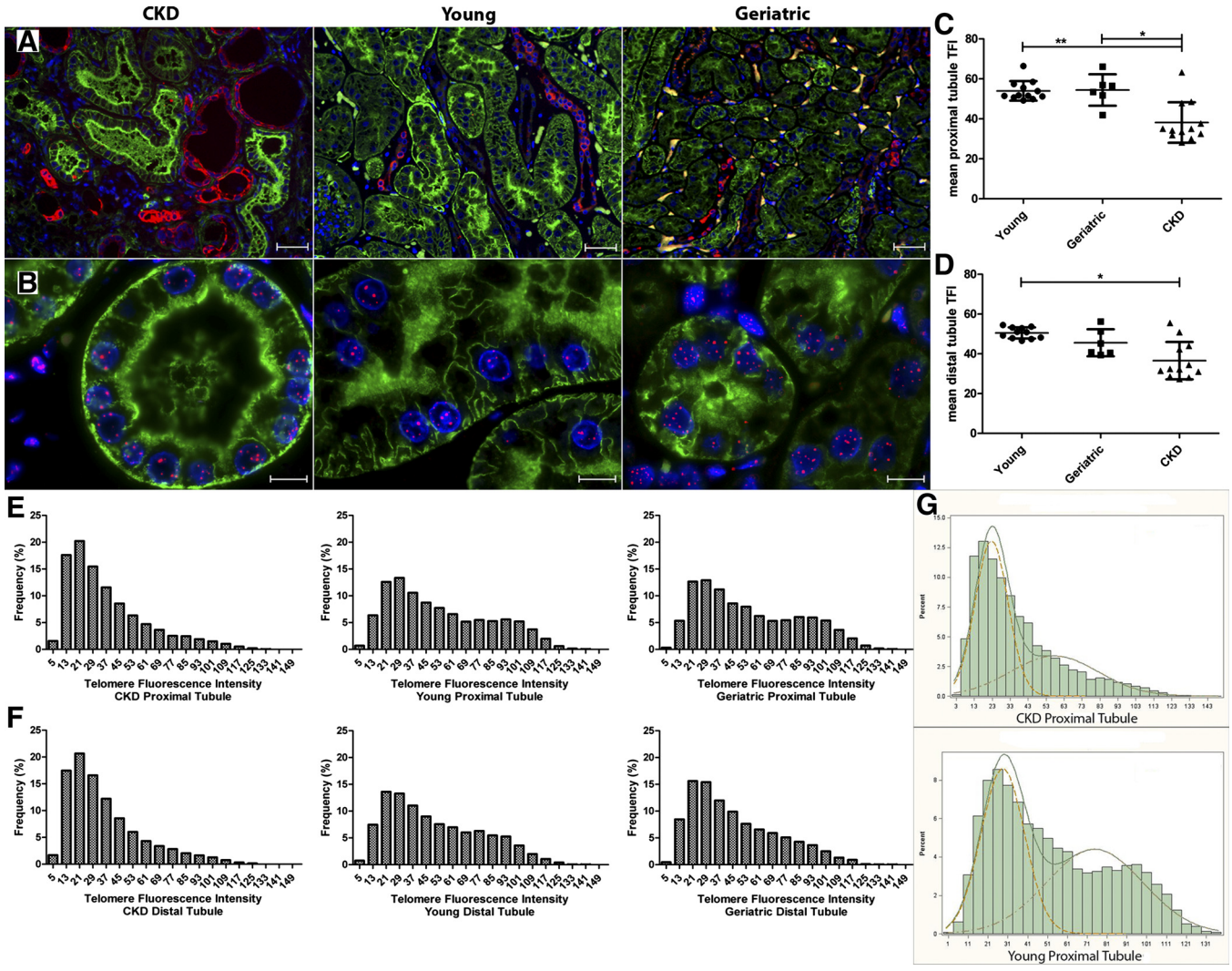

Fig. 1. Telomere length analysis of feline kidneys. *A*: telomere fluorescent in situ hybridization combined with immunohistochemistry (TELI-FISH) of renal cortex in chronic kidney disease (CKD; *left*), young normal (*middle*), and geriatric normal (*right*) cats. Aquaporin 1-positive proximal tubules are stained green, cytokeratin-positive distal tubules are red, and nuclei are blue (×20 magnification; scale bar represents 30 μm). Loss of proximal tubules is apparent in CKD cats. *B*: renal cortex at ×100 magnification. Telomeric signals are in red. Scale bar represents 5 μm. *C*: average telomere fluorescence intensity (TFI) of proximal tubular epithelial cells. Using a one-way ANOVA with Dunn's post hoc analysis, a statistically significant decrease in the average TFI of proximal tubular epithelial cells of CKD cats compared with young normal and geriatric normal cats was demonstrated ($P = 0.0007$). *D*: average TFI of distal tubular epithelial cells. Using a one-way ANOVA with Dunn's post hoc analysis, a statistically significant decrease in the average TFI of distal tubular epithelial cells of CKD cats compared with young normal and geriatric normal cats was demonstrated ($P = 0.004$). *E*: proximal tubule individual TFI frequency histograms. A statistically significant decrease in the individual TFI of proximal tubular epithelial cells of CKD cats [mean: 36.9; confidence interval (CI): 36.4–37.4] is demonstrated compared with young normal (mean: 53.0; CI: 52.4–53.8) and geriatric normal cats (mean: 54.2; CI: 53.2–55). *F*: distal tubule individual TFI frequency histograms. A statistically significant decrease in the individual TFI of distal tubular epithelial cells of CKD cats (mean: 36.9; CI: 36.4–37.4) is demonstrated compared with young normal (mean: 53.0; CI: 52.4–53.8) and geriatric normal cats (mean: 54.2; CI: 53.2–55). *G*: finite mixed-model analysis of bimodal distribution present in proximal tubule frequency histogram. Two distributions (A = low end; B = high end) were isolated from the histogram. Individual distributions in the CKD cat group (mean A ± SE = 22.6 ± 0.24; mean B = 57.6 ± 0.78) were significantly different from those in young normal (mean A = 28.4 ± 0.44; mean B = 74.9 ± 1.1) and normal geriatric (mean A = 29.1 ± 0.57; mean B = 76.6 ± 1.4) cat groups when compared with a *t*-test ($P = < 0.05$). Distribution B represents unusually large telomere signals that were visually observed in these sample groups.

When histograms of individual kidney TFI (i.e., individual telomeres) were compared, there was a statistically significant decrease in PTEC of CKD cats (mean: 36.9; CI: 36.4–37.4) compared with young normal (mean: 53.0; CI: 52.4–53.8) and geriatric normal cats (mean: 54.2; CI: 53.2–55) (Fig. 1*E*). There was also a statistically significant decrease in the individual TFI of DTEC of CKD cats (mean: 35.8; CI: 35.3–36.2) compared with young normal (mean: 49.9; CI: 49.2–50.6) and geriatric normal cats (mean: 45.7; CI: 44.9–46.3) (Fig. 1*F*). In addition, the distribution of the PTEC histogram was markedly different between CKD and normal cats. A bimodal distribution of TFI signals was apparent in the PTEC histograms of young normal and geriatric normal cats but not in the CKD cats (Fig. 1*E*); this pattern was also apparent in the DTEC histograms, but not as prominently. Further statistical analysis of the histograms with a finite mixed model confirmed its bimodal nature and also allowed comparison of the individual distributions (Fig. 1*G*). Even when the histogram was broken down into two separate distributions (A = low end/short telomeres; B = high end/large telomeres), each individual distribution in the CKD cat group (mean A ± SE = 22.6 ± 0.24; mean B = 57.6 ± 0.78) was significantly different from those in the young normal (mean A = 28.4 ± 0.44; mean B = 74.9 ± 1.1) and geriatric normal (mean A = 29.1 ± 0.57; mean B = 76.6 ± 1.4) cat groups when compared with a *t*-test ($P = < 0.05$). Distribution B represents unusually large telomere signals that were subjectively observed commonly in young normal and geriatric normal sample groups. In CKD cats, it was estimated that only ~40% of the telomere signals were in distribution B, whereas ~53% of the telomere signals in young and old normal cats were in distribution B.

Telomeres are not Shortened in Liver or Skin of Any Group

Standard TEL-FISH was performed on liver and skin sections to assess telomere lengths. Hepatocyte nuclei were identified based on morphological appearance on DAPI images. The basal cell layer of skin samples was identified based on its undulating architecture. No significant difference in average TFI was found for liver or skin samples from any group (Fig. 2, *A* and *C*). When histograms of individual liver TFI were compared, there was a statistically significant increase in the individual TFI of geriatric normal cats (mean: 36; CI: 36–37) compared with young normal (mean: 30; CI: 30–30) and CKD cats (mean: 29; CI: 29–30) (Fig. 2*B*). When histograms of individual skin TFI were compared, there were no statistically significant differences in the individual TFI of CKD cats (mean: 32; CI: 32–33) compared with young normal (mean: 32; CI: 31–32) and old normal cats (mean: 31; CI: 30–31) (Fig. 2*D*). Additionally, no suggestion of bimodal distribution in the frequency histograms for liver or skin was observed, and background autofluorescence was more prominent in the liver of young normal cats than other groups.

Cellular Senescence is Increased in CKD and Geriatric Cat Kidneys

SABG staining was performed on kidney and liver cryosections. Positive blue staining, indicative of senescent cells, was seen prominently in tubular structures in the renal cortex of CKD cats. Some normal geriatric cats also exhibited slight SABG staining of tubules. Representative images from each tissue and group are presented in Fig. 3, *B* and *D*. When analyzed by one-way ANOVA with Dunn's post hoc analysis, a statistically significant increase of SABG staining in kidneys of CKD and geriatric normal cats compared with young normal cats ($P = 0.0001$) was observed (Fig. 3*A*). CKD cat kidneys tended to have increased SABG staining compared with normal geriatric cats, but this did not reach statistical significance. Minimal SABG staining was seen in liver samples compared with kidney; however, CKD cats did have a statistically significant increase in staining in liver compared with other groups (Fig. 3*C*).

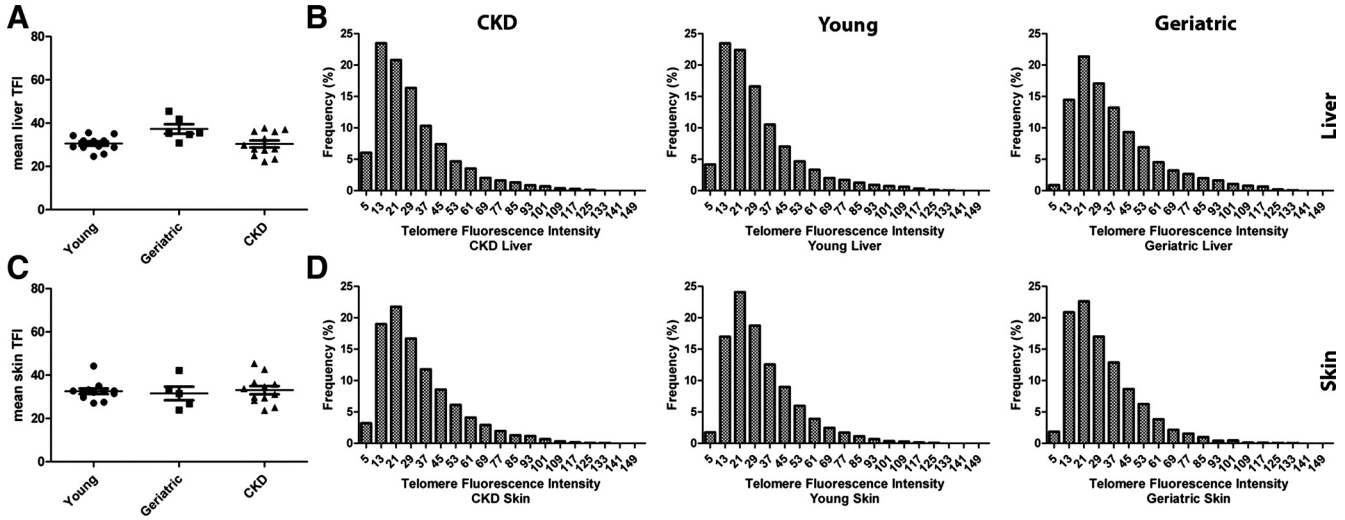

Fig. 2. Telomere length analysis of feline liver and skin. *A*: average TFI of hepatocytes. Using a one-way ANOVA with Dunn's post hoc analysis, no significant difference in the average TFI of hepatocytes between groups was demonstrated. *B*: hepatocyte individual TFI frequency histograms. There was a statistically significant increase in the individual TFI of geriatric normal cats (mean: 36; CI: 36–37) compared with young normal (mean: 30; CI: 30–30) and CKD cats (mean: 29; CI: 29–30) ($P = < 0.05$). *C*: average TFI of skin cells. Using a one-way ANOVA with Dunn's post hoc analysis, no significant difference in the average TFI of skin cells between groups was demonstrated. *D*: skin individual TFI frequency histograms. No statistically significant difference is noted between cat groups.

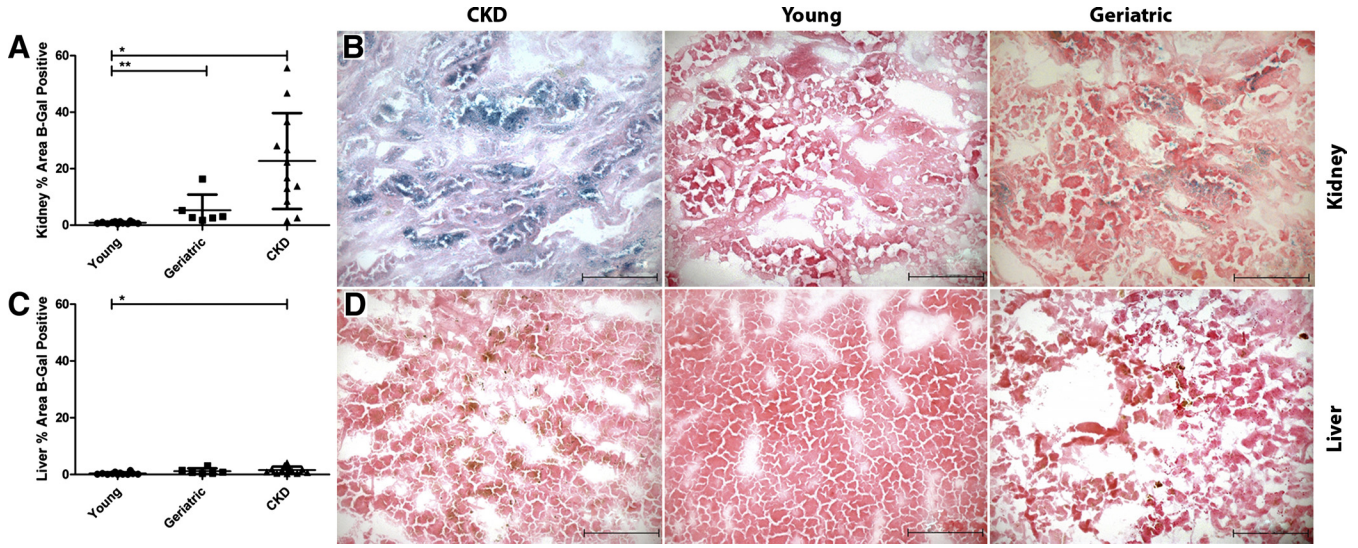

Fig. 3. Assessment of senescence with senescence-associated β-galactosidase (SABG) staining. *A*: image analysis of SABG staining in feline kidney. Analysis of percent area positive was performed for four images from each sample, and an average was calculated. There was a statistically significant increase in SABG staining in CKD kidney samples compared with young normal cats ($P = 0.0001$). CKD cats tended to have increased SABG staining compared with normal geriatric cats, but this did not reach statistical significance. *B*: SABG staining in renal cortex of CKD cats (*left*), young normal cats (*middle*), and normal geriatric cats (*right*) (×20 magnification). Scale bar represents 100 μm. *C*: image analysis of SABG staining in the liver. Analysis of percent area positive was performed for four images from each sample, and an average was calculated. Minimal SABG staining was seen in liver samples compared with kidney; however, the CKD cats had a statistically significant increase in staining compared with other groups. *D*: SABG staining in liver of CKD cats (*left*), young normal cats (*middle*), and normal geriatric cats (*right*) (×20 magnification). Scale bar represents 100 μm.

Telomerase Activity is Present in Kidney and Liver Samples from All Groups

RTQ-TRAP was used to analyze telomerase activity in feline liver and kidney samples from a subset of five cats from each group (Fig. 4). Telomerase activity was detected in all tissues by this sensitive approach. When analyzed by one-way ANOVA with Dunn's post hoc analysis, no statistically significant differences in kidney telomerase activity were observed for any of the groups. A statistically significant increase in telomerase activity was observed in the liver of CKD cats compared with young normal and geriatric normal cat livers ($P < 0.05$).

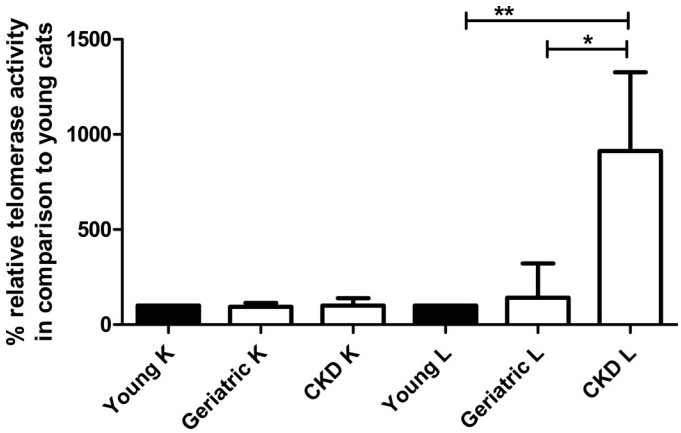

Fig. 4. Real-time quantitative telomeric repeat amplification protocol measurement of relative telomerase activity in feline kidney and liver. Telomerase activity was evaluated in liver and kidney samples from a subset of five cats in each study group. Relative telomerase activity was determined by normalization to the average telomerase activity for each tissue from young normal cats. Telomerase activity, although low, was detected in all feline tissues from all groups. When analyzed by one-way ANOVA with Dunn's post hoc analysis, no significant difference in kidney telomerase activity was detected between groups. A statistically significant increase in telomerase activity was observed in the liver of CKD cats compared with young normal and geriatric normal cat livers ($P < 0.05$).

DISCUSSION

We provide the first evidence of shortened telomeres and increased cellular senescence in the kidneys of cats with CKD. A novel approach was adapted for use in feline kidneys to facilitate cell-by-cell analysis of telomere length in specific cellular compartments within the renal cortex. Analysis of telomere length in both PTEC and DTEC populations demonstrated that they were significantly shorter (up to two times) in cats with CKD compared with either young normal cats or geriatric cats without indication of CKD. Significant diminution of telomere lengths was not observed in the liver or skin, which were used as control organs. Additionally, increased cellular senescence was documented in the kidneys of cats with CKD compared with young normal cats. Increased cellular senescence was also found in the kidneys of normal geriatric cats, although not to the degree present in CKD cats, and so was consistent with normal aging. Overall, minimal cellular senescence was observed in liver samples compared with kidney.

The renal environment in CKD is compromised by processes such as inflammation, intraglomerular hypertension, hypoxia, and oxidative stress (12, 35, 42). In human CKD patients, increased systemic oxidative stress has been documented as a result of increased oxidant activity and reduced antioxidant capacity (20, 25, 39). Similar findings have been documented in cats with CKD (21, 50). Telomeres are known to be sensitive to oxidative stress, and replication combined with an impaired ability to repair oxidative damage causes rapid telomere shortening and dysfunction (16). Thus it is perhaps not surprising

that telomeres are shortened in CKD cats, an observation also consistent with previous reports in other species. For example, oxidative stress, hypertension, and renal ischemia have been shown to be associated with shortened renal telomeres in rats (11, 19, 46). Therefore, oxidative stress may be an important mechanism by which telomeres become prematurely shortened in cats. Additional studies are needed to explore the correlation between renal oxidative stress, telomere length, and cellular senescence in CKD patients. The finding of increased renal cellular senescence has also been previously demonstrated in human aging and disease (32, 33, 48). As is seen with inflammatory conditions in other organs, a continued environment of inflammation and cellular damage present in the kidney could result in increased cellular replication and repair, leading to telomere shortening and eventual replicative senescence (1, 28). Replicative senescence would be difficult to differentiate from oxidative stress-induced telomere shortening as a definitive mechanism for underlying association between telomeres, senescence, and CKD. More than likely, the pathophysiology is multifactorial in nature, with both processes having the potential to contribute to the progression of disease.

A few human studies have examined the relationship between age and renal telomere attrition and concluded that telomeres shorten in an age-dependent manner, particularly in the renal cortex (31, 47). In cats, telomere length in relation to age has been investigated by telomere restriction fragment (TRF) analysis of peripheral blood mononuclear cells (PBMC); a significant decrease in PBMC telomere length was found with increasing age (29). In the present study, age alone did not appear to result in significant telomere shortening in the kidney or liver. This finding could reflect clustering/association of critically short telomeres, so they are lost to the analysis, and/or the ages of the cats in our sample groups, and/or the relatively small number of cats in the study, particularly geriatric cats with no evidence of CKD. Larger cohort size and a greater range of ages would be necessary to more thoroughly investigate and conclusively establish the effect of age on renal telomere length. Normal geriatric cats had slightly higher TFI in the liver than normal young cats, at least some of which may be attributable to technical issues, such as higher background autofluorescence in young normal cats compared with other samples, which would affect telomere intensity signals by decreasing their measurable value.

The SABG staining employed to evaluate senescence can only be performed on cryosection samples, so parenchymal architecture was not as well preserved as in the paraffin-embedded samples. Therefore, it was sometimes challenging to accurately resolve which cells were SABG positive, since different cellular compartments were difficult to distinguish and individual tubular cells could not be identified; SABG positive tubular structures were confirmed with aquaporin 1 immunohistochemistry. Future feline CKD studies will require measurement of senescence on paraffin-embedded tissues so that a better assessment of precisely which cells are senescent can be made. Similar to our telomere length analysis, the small number of cats in the normal geriatric group likely limited our ability to thoroughly assess the relationship between renal age and senescence. Although subjectively there appears to be a difference in the degree of senescence between CKD cats and normal geriatric cats (Fig. 3*B*), the difference did not reach statistical significance. It should also be noted that, although the large variance in CKD cat senescence values affected the ability to detect significant differences between groups, it is in fact the shortest individual telomeres that are the critical ones, since it takes only one/few to trigger senescence.

Telomerase activity, evaluated by RTQ-TRAP, was observed in feline kidney and liver samples from all groups in this study. When tissue levels were compared with HeLa cell lysate (positive control) run at the same protein concentration, the kidney and liver had 15.2% and 2.5%, respectively, of the telomerase activity seen in the HeLa cell lysate (data not shown). These findings are inconsistent with previous studies in cats where telomerase activity was not observed in normal somatic tissues (4, 29). The most likely explanation for this difference is the increased sensitivity of the RTQ-TRAP assay over traditional TRAP assays. The RTQ-TRAP assay measures, via quantitative real-time PCR instrumentation (i.e., CFX96), SYBR green incorporation into newly elongated DNA, in this case telomere repeat sequences. The measurable changes in SYBR-green incorporation are exponentially more sensitive and precise than the detection methods utilized in traditional TRAP techniques (22, 23). As a result, cells or tissues once considered negative for telomerase are demonstrating telomerase activity when remeasured using the RTQ-TRAP method, as is the case with these feline tissues.

Feline kidney telomerase activity was low but very comparable between young normal, geriatric normal, and CKD cats. This finding has potential and important therapeutic implications based on recent intriguing work on the tissue-regenerative effects of telomerase reactivators (17). In contrast to the kidney, a statistically significant increase in telomerase activity in the liver of CKD cats was observed, even though all liver samples were histopathologically normal and no cats had elevated liver enzymes or serum biochemistry. Although the liver is not the focus of this study, one postulated explanation for this finding is that systemic oxidative stress observed in CKD cats could be modulating antioxidant mechanisms in the liver that might result in elevating liver telomerase levels. Previous work has implied a connection between oxidative stress and increased telomerase activity (26). Further studies are needed to explore this potential relationship.

Individual TFI histograms revealed significant variability in the size of PTEC telomere signals in young and old normal cats; bimodal distributions were readily appreciated. PTEC tended to have one to two rather large telomere signals in additional to several smaller ones. This phenomenon was not observed in CKD cats or liver or skin samples from any of the groups. This potentially could be a technical phenomenon where individual telomeres appear clumped together in the compressed deconvoluted picture. However, 3D reconstructions serve to circumvent this issue, and indeed when 3D images were created, the larger telomere signals persisted. The simplest explanation might well be the most probable, in that the larger signals observed in the young cats likely represent long telomeres associated with youth, whereas in the geriatric cats they represent associations or aggregates of short telomeres resulting from advanced age. Telomere associations are relatively common and have been correlated with increased cancer risk (5). Telomeres do not normally form aggregates, since each telomere has its own 3D space within the cell and does not overlap with other telomeres even during interphase (27). Telomeric aggregates have, however, also been reported,

particularly associated with cancer, and are thought to result from telomere dysfunction (10, 27).

Taken together, the results of this study clearly indicate an association between telomere shortening, cellular senescence, and feline CKD, and even though they do not necessarily demonstrate a cause-and-effect relationship, they do support contribution of telomere dysfunction to progression of disease. Potential mechanisms may involve structural damage to telomeres secondary to oxidative lesions and replicative senescence secondary to continued replication associated with inflammation and damage. Additional unknown factors may well predispose cats to renal insult, the result being continued need for repair and replication, premature telomere shortening, and senescence. Additional investigation is clearly warranted and is necessary to further explore such possibilities and relationships. Importantly, our results also suggest novel intervention strategies and therapeutic targets for treatment of CKD; e.g., amelioration of oxidative stress and/or selective telomerase activation may represent advantageous approaches to combating critical renal telomere shortening, thereby reducing cellular senescence and slowing kidney degeneration (8, 17, 44).

ACKNOWLEDGMENTS

The authors thank Dr. Alan Meeker for consultation regarding methodology, Dr. James zumBrunnen for assistance with statistical analysis, Dr. Joel Bedford for microscope access, and Lauren Habenicht for assistance with data entry.

GRANTS

This study was funded by a grant from the Morris Animal Foundation.

DISCLOSURES

No conflicts of interest, financial or otherwise, are declared by the author(s).

AUTHOR CONTRIBUTIONS

Author contributions: J.M.Q. and S.M.B. conception and design of research; J.M.Q., D.G.M., C.L.B., S.M.M., and W.T.B. performed experiments; J.M.Q. and C.L.B. analyzed data; J.M.Q. and C.L.B. interpreted results of experiments; J.M.Q. and W.T.B. prepared figures; J.M.Q. drafted manuscript; J.M.Q., D.G.M., C.L.B., S.M.M., and S.M.B. edited and revised manuscript; J.M.Q., D.G.M., C.L.B., S.M.M., and S.M.B. approved final version of manuscript.

REFERENCES

1. **Aikata H, Takaishi H, Kawakami Y, Takahashi S, Kitamoto M, Nakanishi T, Nakamura Y, Shimamoto F, Kajiyama G, Ide T.** Telomere reduction in human liver tissues with age and chronic inflammation. *Exp Cell Res* 256: 578–582, 2000.
2. **Boyd LM, Langston C, Thompson K, Zivin K, Imanishi M.** Survival in cats with naturally occurring chronic kidney disease (2000–2002). *J Vet Intern Med* 22: 1111–1117, 2008.
3. **Brandt LE, Bohn AA, Charles JB, Ehrhart EJ.** Localization of canine, feline, and mouse renal membrane proteins. *Vet Pathol* 49: 693–703, 2011.
4. **Cadile CD, Kitchell BE, Biller BJ, Hetler ER, Balkin RG.** Telomerase activity as a marker for malignancy in feline tissues. *Am J Vet Res* 62: 1578–1581, 2001.
5. **Cottliar A, Fundia A, Boerr L, Sambuelli A, Negreira S, Gil A, Gomez JC, Chopita N, Bernedo A, Slavutsky I.** High frequencies of telomeric associations, chromosome aberrations, and sister chromatid exchanges in ulcerative colitis. *Am J Gastroenterol* 95: 2301–2307, 2000.
6. **DiBartola SP, Rutgers HC, Zack PM, Tarr MJ.** Clinicopathologic findings associated with chronic renal disease in cats: 74 cases (1973–1984). *J Am Vet Med Assoc* 190: 1196–1202, 1987.
7. **Dimri GP, Lee X, Basile G, Acosta M, Scott G, Roskelley C, Medrano EE, Linskens M, Rubelj I, Pereira-Smith O, et al.** A biomarker that identifies senescent human cells in culture and in aging skin in vivo. *Proc Natl Acad Sci USA* 92: 9363–9367, 1995.
8. **Feng X, Wang L, Li Y.** Change of telomere length in angiotensin II-induced human glomerular mesangial cell senescence and the protective role of losartan. *Mol Med Report* 4: 255–260, 2011.
9. **Fusaro L, Panarese S, Brunetti B, Zambelli D, Benazzi C, Sarli G.** Quantitative analysis of telomerase in feline mammary tissues. *J Vet Diagn Invest* 21: 369–373, 2009.
10. **Goldberg-Bittman L, Kitay-Cohen Y, Quitt M, Hadary R, Fejgin MD, Yukla M, Amiel A.** Telomere aggregates in non-Hodgkin lymphoma patients at different disease stages. *Cancer Genet Cytogen* 184: 105–108, 2008.
11. **Hamet P, Thorin-Trescases N, Moreau P, Dumas P, Tea BS, deBlois D, Kren V, Pravenec M, Kunes J, Sun Y, Tremblay J.** Workshop: excess growth and apoptosis: is hypertension a case of accelerated aging of cardiovascular cells? *Hypertension* 37: 760–766, 2001.
12. **Harris RC, Neilson EG.** Toward a unified theory of renal progression. *Annu Rev Med* 57: 365–380, 2006.
13. **Herbert BS, Hochreiter AE, Wright WE, Shay JW.** Nonradioactive detection of telomerase activity using the telomeric repeat amplification protocol. *Nat Protoc* 1: 1583–1590, 2006.
14. **Hirota J, Usui R, Satoh T, Ikemoto S.** Telomere position on the cat chromosome. *J Vet Med Sci* 58: 1025–1026, 1996.
15. **Hou M, Xu D, Bjorkholm M, Gruber A.** Real-time quantitative telomeric repeat amplification protocol assay for the detection of telomerase activity. *Clin Chem* 47: 519–524, 2001.
16. **Houben JM, Moonen HJ, van Schooten FJ, Hageman GJ.** Telomere length assessment: biomarker of chronic oxidative stress? *Free Radic Biol Med* 44: 235–246, 2008.
17. **Jaskelioff M, Muller FL, Paik JH, Thomas E, Jiang S, Adams AC, Sahin E, Kost-Alimova M, Protopopov A, Cadinanos J, Horner JW, Maratos-Flier E, Depinho RA.** Telomerase reactivation reverses tissue degeneration in aged telomerase-deficient mice. *Nature* 469: 102–106, 2011.
18. **Jiang H, Ju Z, Rudolph KL.** Telomere shortening and ageing. *Z Gerontol Geriatr* 40: 314–324, 2007.
19. **Joosten SA, van Ham V, Nolan CE, Borrias MC, Jardine AG, Shiels PG, van Kooten C, Paul LC.** Telomere shortening and cellular senescence in a model of chronic renal allograft rejection. *Am J Pathol* 162: 1305–1312, 2003.
20. **Kao MP, Ang DS, Pall A, Struthers AD.** Oxidative stress in renal dysfunction: mechanisms, clinical sequelae and therapeutic options. *J Hum Hypertens* 24: 1–8, 2010.
21. **Keegan RF, Webb CB.** Oxidative stress and neutrophil function in cats with chronic renal failure. *J Vet Intern Med* 24: 514–519, 2010.
22. **Kim NW, Piatyszek MA, Prowse KR, Harley CB, West MD, Ho PLC, Coviello GM, Wright WE, Weinrich SL, Shay JW.** Specific association of human telomerase activity with immortal cells and cancer. *Science* 266: 2011–2015, 1994.
23. **Kim NW, Wu F.** Advances in quantification and characterization of telomerase activity by the telomeric repeat amplification protocol (TRAP). *Nucleic Acids Res* 25: 2595–2597, 1997.
24. **Livak KJ, Schmittgen TD.** Analysis of relative gene expression data using real-time quantitative PCR and the 2(-delta delta C(T)) method. *Methods* 25: 402–408, 2001.
25. **Locatelli F, Canaud B, Eckardt KU, Stenvinkel P, Wanner C, Zoccali C.** Oxidative stress in end-stage renal disease: an emerging threat to patient outcome. *Nephrol Dial Transplant* 18: 1272–1280, 2003.
26. **Lopez-Diazguerrero NE, Perez-Figueroa GE, Martinez-Garduno CM, Alarcon-Aguilar A, Luna-Lopez A, Gutierrez-Ruiz MC, Konigsberg M.** Telomerase activity in response to mild oxidative stress. *Cell Biol Int* 36: 409–413, 2012.
27. **Mai S, Garini Y.** The significance of telomeric aggregates in the interphase nuclei of tumor cells. *J Cell Biochem* 97: 904–915, 2006.
28. **Masi S, Salpea KD, Li K, Parkar M, Nibali L, Donos N, Patel K, Taddei S, Deanfield JE, D'Aiuto F, Humphries SE.** Oxidative stress, chronic inflammation, and telomere length in patients with periodontitis. *Free Radic Biol Med* 50: 730–735, 2011.
29. **McKevitt TP, Nasir L, Wallis CV, Argyle DJ.** A cohort study of telomere and telomerase biology in cats. *Am J Vet Res* 64: 1496–1499, 2003.
30. **Meeker AK, Gage WR, Hicks JL, Simon I, Coffman JR, Platz EA, March GE, De Marzo AM.** Telomere length assessment in human archival tissues: combined telomere fluorescence in situ hybridization and immunostaining. *Am J Pathol* 160: 1259–1268, 2002.

31. **Melk A, Ramassar V, Helms LM, Moore R, Rayner D, Solez K, Halloran PF.** Telomere shortening in kidneys with age. *J Am Soc Nephrol* 11: 444–453, 2000.
32. **Melk A, Schmidt BM, Takeuchi O, Sawitzki B, Rayner DC, Halloran PF.** Expression of p16INK4a and other cell cycle regulator and senescence associated genes in aging human kidney. *Kidney Int* 65: 510–520, 2004.
33. **Melk A, Schmidt BM, Vongwiwatana A, Rayner DC, Halloran PF.** Increased expression of senescence-associated cell cycle inhibitor p16INK4a in deteriorating renal transplants and diseased native kidney. *Am J Transplant* 5: 1375–1382, 2005.
34. **Naesens M.** Replicative senescence in kidney aging, renal disease, and renal transplantation. *Discov Med* 11: 65–75, 2011.
35. **Nangaku M.** Chronic hypoxia and tubulointerstitial injury: a final common pathway to end-stage renal failure. *J Am Soc Nephrol* 17: 17–25, 2006.
36. **Oeseburg H, de Boer RA, van Gilst WH, van der Harst P.** Telomere biology in healthy aging and disease. *Pflügers Arch* 459: 259–268, 2010.
37. **Perico N, Remuzzi G, Benigni A.** Aging and the kidney. *Curr Opin Nephrol Hypertens* 20: 312–317, 2011.
38. **Pfaffl MW.** A new mathematical model for relative quantification in real-time RT-PCR. *Nucleic Acids Res* 29: e45, 2001.
39. **Popolo A, Autore G, Pinto A, Marzocco S.** Oxidative stress in patients with cardiovascular disease and chronic renal failure. *Free Radic Res* 47: 346–356, 2013.
40. **Reyes JL, Lamas M, Martin D, del Carmen Namorado M, Islas S, Luna J, Tauc M, Gonzalez-Mariscal L.** The renal segmental distribution of claudins changes with development. *Kidney Int* 62: 476–487, 2002.
41. **Risques RA, Lai LA, Brentnall TA, Li L, Feng Z, Gallaher J, Mandelson MT, Potter JD, Bronner MP, Rabinovitch PS.** Ulcerative colitis is a disease of accelerated colon aging: evidence from telomere attrition and DNA damage. *Gastroenterology* 135: 410–418, 2008.
42. **Rodriguez-Iturbe B, Garcia Garcia G.** The role of tubulointerstitial inflammation in the progression of chronic renal failure. *Nephron Clin Pract* 116: 81–88, 2010.
43. **Schmitt R, Coca S, Kanbay M, Tinetti ME, Cantley LG, Parikh CR.** Recovery of kidney function after acute kidney injury in the elderly: a systematic review and meta-analysis. *Am J Kidney Dis* 52: 262–271, 2008.
44. **Smith JA, Park S, Krause JS, Banik NL.** Oxidative stress, DNA damage, and the telomeric complex as therapeutic targets in acute neurodegeneration. *Neurochem Int* 62: 764–775, 2013.
45. **Takubo K, Aida J, Izumiyama-Shimomura N, Ishikawa N, Sawabe M, Kurabayashi R, Shiraishi H, Arai T, Nakamura K.** Changes of telomere length with aging. *Geriatr Gerontol Int* 10, *Suppl* 1: S197–S206, 2010.
46. **Tarry-Adkins JL, Ozanne SE, Norden A, Cherif H, Hales CN.** Lower antioxidant capacity and elevated p53 and p21 may be a link between gender disparity in renal telomere shortening, albuminuria, and longevity. *Am J Physiol Renal Physiol* 290: F509–F516, 2006.
47. **Tchakmakjian L, Gardner JP, Wilson PD, Kimura M, Skurnick J, Zielke HR, Aviv A.** Age-dependent telomere attrition as a potential indicator of racial differences in renal growth patterns. *Nephron Exp Nephrol* 98: 82–88, 2004.
48. **Verzola D, Gandolfo MT, Gaetani G, Ferraris A, Mangerini R, Ferrario F, Villaggio B, Gianiorio F, Tosetti F, Weiss U, Traverso P, Mji M, Deferrari G, Garibotto G.** Accelerated senescence in the kidneys of patients with type 2 diabetic nephropathy. *Am J Physiol Renal Physiol* 295: F1563–F1573, 2008.
49. **von Figura G, Hartmann D, Song Z, Rudolph KL.** Role of telomere dysfunction in aging and its detection by biomarkers. *J Mol Med* 87: 1165–1171, 2009.
50. **Yu S, Paetau-Robinson I.** Dietary supplements of vitamins E and C and beta-carotene reduce oxidative stress in cats with renal insufficiency. *Vet Res Commun* 30: 403–413, 2006.